Development of Omnidirectional Self-Balancing Robot

Hew Yeong Han, Tiong Yih Han, Hudyjaya Siswoyo Jo
Faculty of Engineering, Computing and Science
Swinburne University of Technology Sarawak Campus
Kuching, Malaysia

***Abstract*— The omnidirectional self-balancing robot or otherwise known as ballbot belongs to a special class of balancing robots. With only one contact point with the ground, ballbot is able to achieve a higher degree of agility with a lower footprint than most mobile robots. While practical applications of balancing platforms such as Segway PT have gained much traction over the last decade, directional limitations in movements are still prevalent in wheeled robots. To achieve omnidirectional motion, a ball is used as a replacement to wheels. Similar to the concept of inverted pendulum, self-balancing is achieved using a closed-loop control system. In this paper, we propose the implementation of a minimalist and low cost ball-balancing robot that utilizes off-the-shelf components that are widely available in the market with the aim to create an affordable platform to study and design control strategies for ballbots.**

Keywords—spherical wheel, omni-directional wheel, inverted pendulum.

I. INTRODUCTION

The first ballbot was developed by Lauwers et. al [1] at Carnegie Mellon University (CMU) in 2006 which utilizes the mechanism of an inverse mouse-ball drive. The development was inspired by the idea to sidestep the requirement for human size robots to have wide wheel base to avoid from toppling over during acceleration and deceleration. By incorporating active balancing control, the robot was able to navigate quickly in any directions despite its high center of gravity. Active balancing control allows the attitude of the robot to be continuously corrected to maintain stability.

In 2008, Kumagai and Ochiai [2] introduce several versions of balancing robot which are able to balance itself on a pipe and ball. This was the first ballbot to introduce omnidirectional wheels for its ball drive transmission. The omnidirectional drive consists of three wheels which are aligned at 120° apart through the motor shaft and the contact with the ball is leveled at 40° zenith angle. This wheel arrangement allows the ballbot to achieve on-axis turning. The literature presents the details of the mechanical design of the robot and experimental result, however information related to balancing and control strategies are not clearly reported.

Fankhauser and Gwerder [3] developed a prototype with similar mechanical structure which utilizes omnidirectional wheels as the ball drive mechanism. The robot is modeled as two planar inverted pendulums which are balanced by a linear quadratic state feedback controller (LQR).

Two pioneer researchers in this area, Kumagai and Hollis have been actively researching in different aspects related to the development of ballbot. They have proposed a unique method in tracking and controlling the ball movement using optical mouse sensors [4]. The most recent works involved the development of linear and spherical induction motor for the ball actuation [5] [6].

In general, there are two main challenges to the realization of a ballbot; control strategy and feedback measurement. In most of the existing literatures, the strategy used in controlling a ballbot adopts the two-dimensional inverted pendulum model. The inverted pendulum is to a great extern a classical platform to explore practical control theories since it is inherently unstable. Under gravity, the pendulum would normally fall to the ground. By having feedback from sensors, closed-loop control system can be designed to perform corrections at a high frequency to keep the pendulum upright, hence dynamically stable.

Concurrently, the accuracy of the feedback measurement system is also equally important. The attitude of the robot has to be precisely measured to ensure that corrective actions are accurately applied. As semiconductor technology becomes more affordable, inertial measurement unit (IMU) has become a popular choice for non-contact tilt angle measurements especially in balancing platform. IMU is an attitude sensing module that combines accelerometer and gyroscope to measure changes in orientation based on gravitational force. However extra work has to be done in order to produce the best measurement from the IMU, an algorithm needs to be applied to fuse the accelerometer and gyroscope readings together to perform signal estimation.

The subsequent sections of this paper present the details on the development of the ballbot prototype. Section II discusses the mechanical and electronic system setup of the robot. Section III elaborates on the tilt angle estimation and sensor fusion strategy. Section IV elaborates the kinematics model of the omnidirectional wheels drive as well as the feedback control scheme. Section V presents and discusses the related results obtained from the experiment. Lastly, the conclusion is presented in Section VI.

II. PROTOTYPE SETUP

Fig. 1 shows the fully assembled prototype of the robot. The robot measures 200mm in diameter and 570 mm in height including the ball with the total mass of approximately 4.5kg. The actuation of the robot is provided by three 15W planetary gearhead DC motors. In order to achieve a minimal footprint, the structure of the robot is made up of four circular platforms arranged in layers.

The bottom layer acts as the base of the robot where three omnidirectional wheels attached to each driving motor are arranged at 120° apart at a contact angle of 40° from the horizontal axis. This arrangement allows the wheel to be always in contact with the ball at any given time. To prevent the ball from detaching, three pairs of claw-shaped cages are place around the circumference of the ball. The second layer consists of the motor driving, power circuitry and an 11.1V lithium polymer battery which works as the main power supply for the robot. The third layer houses the control circuit as well as the IMU module for tilt angle measurement and the top layer is a platform for the robot to carry its payload.

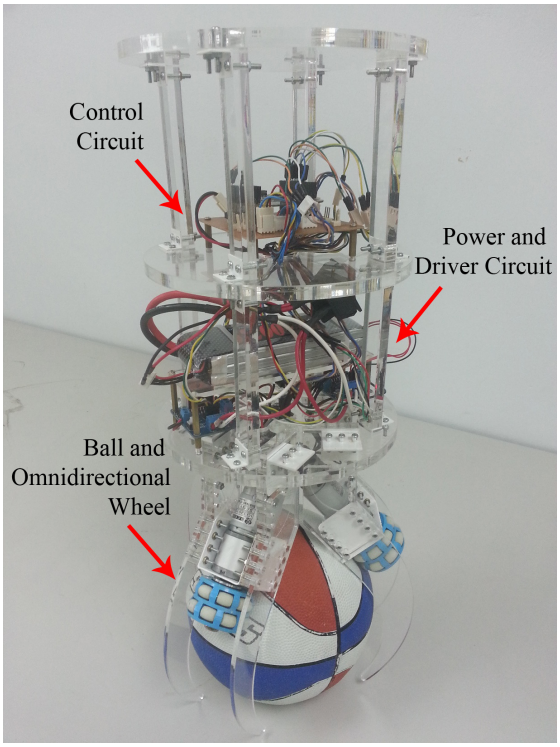

Fig. 1. Prototype of omnidirectional self balancing robot

The control hardware setup is shown in Fig. 2. Freescale ARM 32-bit Freedom Development Board FRDM-KL25Z is used as the main controller for the motion and balancing control. The controller obtains the readings from accelerometer and gyroscope for tilt angle measurement as well as responsible for reading the motors speed from the encoders and applying pulse width modulation (PWM) signal to regulate the speed of the motors

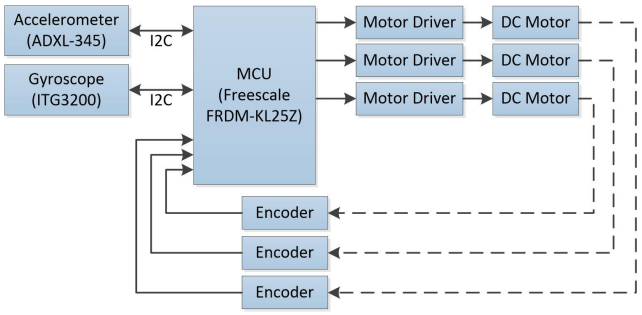

Fig. 2. Block diagram of control system setup

III. TILT ANGLE MEASUREMENT

To monitor the stability of the robot, an IMU is used to measure the pitch and roll angle of the robot. The IMU module consist of Analog Devices ADXL345 3-axis digital accelerometer and Intellisense ITG3200 3-axis gyroscope that each produces a 16-bit output value through I^2C interface. The accelerometer calculates the forces (both gravitational and inertial) exerted on different axis of the sensor based on its orientation. Based on the gravitational force reading obtained, the pitch (φ) and roll (θ) angles can be determined by the trigonometric functions below:

$$\varphi_{accel} = \tan^{-1} \frac{G_y}{\sqrt{G_z^{\,2} + G_x^{\,2}}}$$
$$\theta_{accel} = \tan^{-1} \frac{G_x}{G_z} \qquad (1)$$

The gyroscope provides the measurement of angular rate applied to its body. Therefore, based on the measurement, tilt angles can be obtained by numerically integrating the angular rate values obtained on every sample with the sampling period (t_s):

$$\varphi_{gyro} = \varphi_{gyro} + \dot{\varphi}_{gyro} \times t_s$$
$$\theta_{gyro} = \theta_{gyro} + \dot{\theta}_{gyro} \times t_s \qquad (2)$$

The estimated angles obtained from the accelerometer in (1) are valid only when the accelerometer is experiencing pure angular motion. If the accelerometer is moving at a complex motion, the linear acceleration components will contribute to the error of the estimated angles. On the other hand, the estimated angles obtained from the gyroscope in (2) are immune to linear acceleration as it is only measuring the angular rate. However at stationary position, the output given by the gyroscope tends to drift over time which contributes to the error when the reading is integrated over time.

In order to obtain reliable tilt angle measurements, a complementary filter was used. The complementary filter uses a low pass filter on the accelerometer to reduce the linear acceleration component and high pass filter on the gyroscope reading to eliminate the drift effect.

Low pass filter on accelerometer:

$$\theta_{accel(filt)} = \frac{\tau}{\Delta t + \tau}\theta_{accel(filt)(t-1)} + \frac{\Delta t}{\Delta t + \tau}\theta_{accel}$$

$$\text{let } \frac{\tau}{\Delta t + \tau} = \alpha \text{ and } \frac{\Delta t}{\Delta t + \tau} = 1 - \alpha$$

$$\theta_{accel(filt)} = \alpha\left(\theta_{accel(filt)(t-1)}\right) + (1-\alpha)\theta_{accel} \quad (3)$$

High pass filter on gyroscope:

$$\theta_{\text{gyro}(filt)} = \frac{\tau}{\tau + \Delta t}\left(\theta_{gyro} - \theta_{gyro(t-1)}\right) + \frac{\tau}{\tau + \Delta t}\theta_{\text{gyro}(filt)(t-1)}$$

$$\theta_{\text{gyro}(filt)} = \alpha\left(\theta_{gyro} - \theta_{gyro(t-1)}\right) + \alpha\theta_{\text{gyro}(filt)(t-1)} \quad (4)$$

The filtered values obtained from both sensors in (3) and (4) are summed together to provide more reliable estimation of the robot tilt angle which yields:

$$\theta_{filt} = \theta_{\text{accel}(filt)} + \theta_{\text{gyro}(filt)} \quad (5)$$

Substituting (3) and (4) into (5) yields:

$$\theta_{filt} = \alpha\left(\theta_{accel(filt)(t-1)} + \theta_{gyro(filt)(t-1)} + \dot{\theta}_{gyro} \times \Delta t\right) + (1-\alpha)\theta_{accel} \quad (6)$$

Substituting (5) into (6) yields:

$$\theta_{filt} = \alpha\left(\theta_{filt(t-1)} + \dot{\theta}_{gyro} \times \Delta t\right) + (1-\alpha)\theta_{accel} \quad (7)$$

Coefficient α can be tuned based on the time constant τ, and sampling rate Δt. Based on the iterative experiments during the implementation, α of 0.98 provides the best estimation with minimal noise. The coefficient factor given for gyro measurement is higher than accelerometer because gyroscope readings are more reliable in the short run at higher frequency when the robot is experiencing disturbance. The accelerometer readings only become useful at the steady state and serves as a correction to the accumulated error of the gyroscope. Essentially, the complementary filter aims to solve the predictable weaknesses of both sensors by having each measurement to take precedence after one another at a constant rate determined by the time constant.

IV. Motion and Balancing Control

A. Kinematics Solution of Ball Drive

The desired motion of the robot is solely achieved by varying the speed of each wheel accordingly. To find the desired speed for all the three wheels ($\omega_1, \omega_2, \omega_3$), three known variables have to be provided i.e. speed in x direction (v_x), speed in y direction (v_y) and rotational speed about the robot body (ω_O).

The inverse kinematics can be solved by utilizing force coupling matrix. Fig. 3 shows the free body diagram of the wheel arrangement.

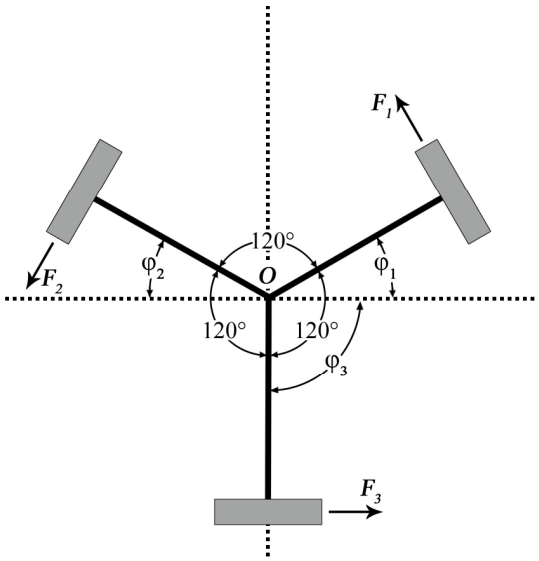

Fig. 3. Free body diagram of delta wheel arrangement

Resolving forces into x and y components:

$$\begin{aligned} Ma_x &= -F_1\sin\varphi_1 - F_2\sin\varphi_2 + F_3\sin\varphi_3 \\ Ma_y &= F_1\cos\varphi_1 - F_2\cos\varphi_2 - F_3\cos\varphi_3 \end{aligned} \quad (8)$$

Taking the torque about point O:

$$\begin{aligned} \tau_O &= I\alpha \\ R\left(F_1 + F_2 + F_3\right) &= MR^2\alpha_O \\ MR\alpha_O &= F_1 + F_2 + F_3 \end{aligned} \quad (9)$$

Substituting $\varphi_1 = \varphi_2 = 30°$ and $\varphi_3 = 90°$ into (8) and (9):

$$\begin{aligned} Ma_x &= -\frac{1}{2}F_1 - \frac{1}{2}F_2 + F_3 \\ Ma_y &= \frac{1}{2}\sqrt{3}F_1 - \frac{1}{2}\sqrt{3}F_2 \\ MR\alpha_O &= F_1 + F_2 + F_3 \end{aligned} \quad (10)$$

Arranging (10) in matrix form yields:

$$\begin{bmatrix} Ma_x \\ Ma_y \\ MR\alpha_O \end{bmatrix} = \begin{bmatrix} -0.5 & -0.5 & 1 \\ 0.866 & -0.866 & 0 \\ 1 & 1 & 1 \end{bmatrix} \begin{bmatrix} F_1 \\ F_2 \\ F_3 \end{bmatrix} \quad (11)$$

Taking inverse of (11) yields:

$$\begin{bmatrix} F_1 \\ F_2 \\ F_3 \end{bmatrix} = \begin{bmatrix} -0.33 & 0.58 & 0.33 \\ -0.33 & -0.58 & 0.33 \\ 0.67 & 0 & 0.33 \end{bmatrix} \begin{bmatrix} Ma_x \\ Ma_y \\ MR\alpha_O \end{bmatrix}$$

$$\begin{aligned} F_1 &= -0.33Ma_x + 0.58Ma_y + 0.33MR\alpha_O \\ F_2 &= -0.33Ma_x - 0.58Ma_y + 0.33MR\alpha_O \\ F_3 &= 0.67Ma_x + 0.33MR\alpha_O \end{aligned} \quad (12)$$

Let acceleration of the wheel $a = r_{wheel}\dot{\omega}$ and substituting it to (12):

$$\begin{aligned} Mr_{wheel}\dot{\omega}_1 &= -0.33Ma_x + 0.58Ma_y + 0.33MR\alpha_O \\ Mr_{wheel}\dot{\omega}_2 &= -0.33Ma_x - 0.58Ma_y + 0.33MR\alpha_O \\ Mr_{wheel}\dot{\omega}_3 &= 0.67Ma_x + 0.33MR\alpha_O \end{aligned} \quad (13)$$

Simplifying and taking integral over time on (13) yields:

$$\begin{aligned} \omega_1 &= \frac{-0.33v_x + 0.58v_y + 0.33R\omega_O}{r_{wheel}} \\ \omega_2 &= \frac{-0.33v_x - 0.58v_y + 0.33R\omega_O}{r_{wheel}} \\ \omega_3 &= \frac{0.67v_x + 0.33R\omega_O}{r_{wheel}} \end{aligned} \quad (14)$$

Given the desired linear and yaw speeds (v_x, v_y and ω_O), the required speed of the wheel can be found by the inverse kinematics solutions in (14).

B. Balancing Control System

The omnidirectional balancing control of the robot is divided into two axis planes in the x and y directions. Using this method, the propulsion is simplified to two virtual wheels that move in the x and y directions. The IMU constantly measures the magnitude and direction of the tilt angle. From the angles obtained, PID control is applied separately at the pitch and roll axis in order to determine the accelerations that are required in both x and y directions. The controller then accelerates the robot towards the direction of tilt by actuating the three wheels based on the inverse kinematics equation derived in the previous section. With the rest angle set at 0°, the closed-loop controller will constantly actuate the ball to maintain its balance. In the implementation, the process is iterated at the rate of 100Hz and the robot is dynamically balanced during runtime.

The main reason PID controller is adopted in this system is due to its simplicity. Because accurate mathematical model of the robot is not readily available, a black-box control strategy is used by tuning the plant experimentally. The diagram in Fig. 4 shows the control block diagram implemented in both roll and pitch angle control.

The PID gains were tuned intuitively by observing the changes in behavior of the plant. During implementation, the output windup caused by the integral term induced a lag in the system because of the integration of error over time. The problem was solved by introducing a velocity mode PID control in place of the usual position control mode. This eliminates the requirement to include integral summation of the error for the I-term.

For the error of pitch and roll angle as follows:

$$\varphi_{err} = \varphi_{meas} - 0° \text{ and } \theta_{err} = \theta_{meas} - 0° \quad (15)$$

The algorithm for the control system is hence:

$$\begin{aligned} V_\varphi &= V_{\varphi(t-1)} + K_P(\varphi - \varphi_{t-1}) + K_I(\varphi) + K_D(\varphi - 2\varphi_{t-1} + \varphi_{t-2}) \\ V_\theta &= V_{\theta(t-1)} + K_P(\theta - \theta_{t-1}) + K_I(\theta) + K_D(\theta - 2\theta_{t-1} + \theta_{t-2}) \end{aligned} \quad (16)$$

Equation (16) expresses the control equation to maintain the robot in the upright position, φ is the inclination of the robot in the pitch axis and θ is the pitch angle of the robot. The subscript t-1 refers to the previous iteration and t-2 refers to two iterations before the current ones. The gains K_P, K_I and K_D are tuned experimentally. The output for each control loop is the output velocity of the ball in the x and y axis. The proportion of tilt in the pitch and roll axis determines the direction of tilt. Thus, the algorithm ensures that control outputs are proportional to the tilt magnitude so that the robot moves to the direction of tilt. When the control outputs for both the pitch and roll axis are obtained, the inverse kinematics equation will determine the speed required for each wheels to move towards the correct direction. Separately, the speeds of the three motors are regulated in an inner closed-loop controller based on the feedback obtained from the quadrature encoders. The diagram in Fig. 5 outlines the regulation method for the motor. The feedback speed measured from the encoder ensures that the right amount of voltage is applied to the motor via PWM to achieve the desired speed.

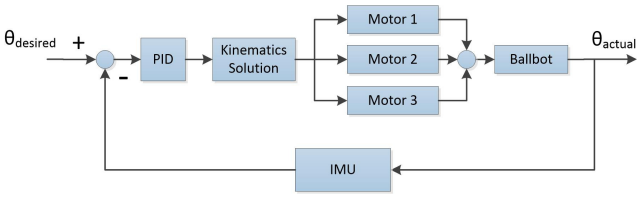

Fig. 4. Block diagram of tilt balancing control

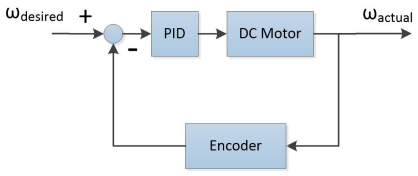

Fig. 5. Block diagram of motor speed control

V. EXPERIMENTAL RESULTS

From the experiments, the PID gains combination that was observed to produce the best results was K_P=10, K_I=1.5 and K_D=20. The tilt angles were recorded from the IMU when the robot was balancing itself. Fig. 6 shows the tilt angles of the robot when performing self-balancing action. The oscillation of the robot was maintained at a magnitude of less than 2° which appears dynamically stable in the physical plant. When extra payload was added the results show no visible change with only small fluctuation during loading and unloading. The robot can hold a maximum of 1 kg load before reaching its saturation point.

The position of the robot is also calculated in balancing mode by the forward kinematics formula derived earlier using the displacement recorded by the encoders in each motor. Fig. 7 shows the scatter plot of the robot's position in Cartesian coordinate. Under small oscillation back and forth, the robot maintained its position with small fluctuation of not more than 40mm away from its center point as shown in the plot.

The ballbot also demonstrates the ability to recover from external disturbance force applied to the body. Fig. 8 shows the plot of the tilt angles with external disturbance applied by pushing the robot by hand. The circles in the plot shows the point when disturbance is applied to the robot and it was able to recover to its upright position. Due to the limitation of the actuators, the robot can handle a maximum of 5 degrees tilt and a small amount of force.

The advantage of using the ball acceleration as the control output is robustness to changes of inertia. In the test result, the robot is able to adapt to changes in weight when tested with additional loads. Besides, it is also much simpler to control the velocity of motors instead of torque. Dividing the control to two different axis planes also greatly simplifies the overall model. Compared to a complex 3D model control, the strategy that we used is more intuitive and easily understood which makes tuning a lot easier.

VI. CONCLUSION

The paper discusses the design and development of omnidirectional self-balancing robot with spherical wheel drive. Details on mechanical and electronic system design, tilt angle estimation method as well as motion and balancing control strategies are presented.

The experimental results show that the developed control strategy allows the robot to dynamically maintain its balance. In addition, the robot is also able to recover from the tilt resulted from the external disturbance applied.

REFERENCES

[1] T. B. Lauwers, G. A. Kantor, R. L. Hollis, "A dynamical stable single-wheeled mobile robot with inverse mouse-ball drive," Proceedings of IEEE International Conference on Robotics and Automation, pp. 2884-2889, May 2006.

[2] M. Kumagai and T. Ochiai, "Development of a robot balancing on a ball," Proceedings of International Conference on Control, Automation and Systems, pp. 433-438, Oct 2008.

[3] P. Fankhauser and C. Gwerder, "Modeling and control of a ballbot," Bachelor thesis, ETH Zurich, 2010.

[4] M. Kumagai and R.L. Hollis, "Development of a three-dimensional ball rotation sensing system using optical mouse sensors," Proceedings of IEEE International Conference on Robotics and Automation, pp. 5038-5043, May 2011.

[5] M. Kumagai and R.L. Hollis, " Development and control of a three DOF planar induction motor," Proceedings of IEEE International Conference on Robotics and Automation, pp. 3757-3762, May 2012.

[6] M. Kumagai and R.L. Hollis, " Development and control of a three DOF spherical induction motor," Proceedings of IEEE International Conference on Robotics and Automation, pp. 1528-1533, May 2013.

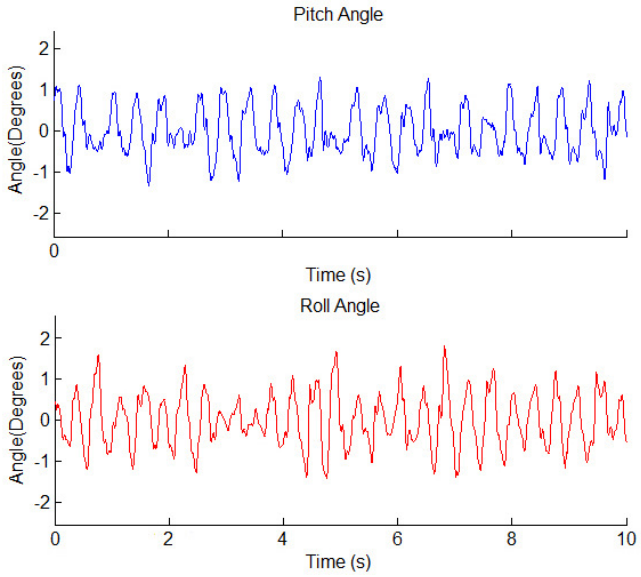

Fig. 6. Measured tilt angles with no external disturbance applied

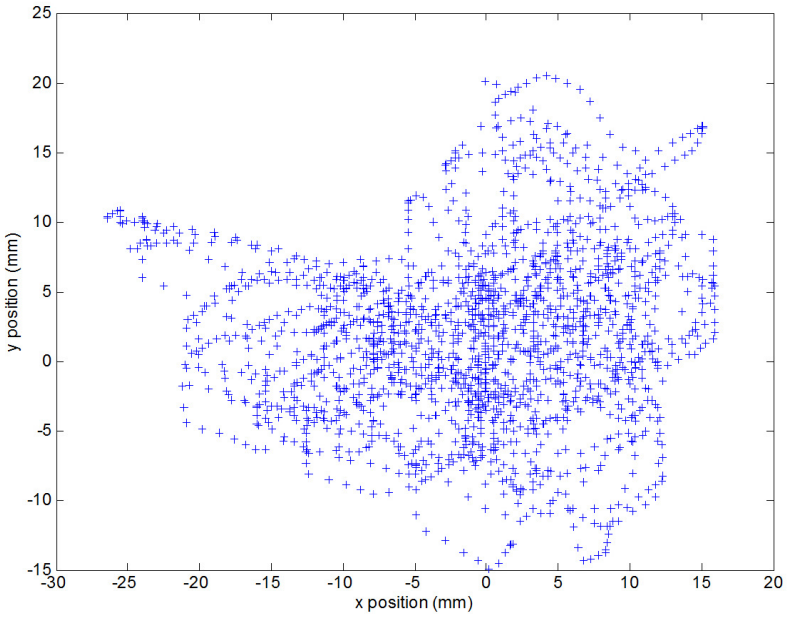

Fig. 7. Robot position in transverse plane for 10 seconds during self-balancing

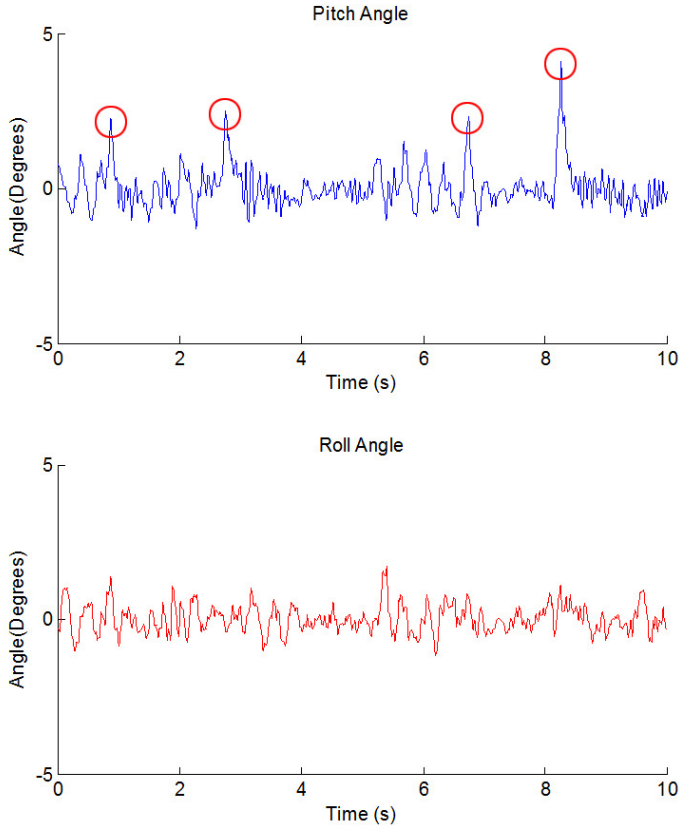

Fig. 8. Measured tilt angles with external disturbance applied